Rotation driven by fast ions in tokamaks

A. Thyagaraja
EURATOM/UKAEA Fusion Association, Culham Science Centre, Abingdon OX14 3DB, United Kingdom

F. Schwander
Department of Aeronautics, Imperial College London, London SW7 2AZ, United Kingdom

K. G. McClements
EURATOM/UKAEA Fusion Association, Culham Science Centre, Abingdon OX14 3DB, United Kingdom

(Received 17 July 2007; accepted 2 October 2007; published online 8 November 2007)

Collective fast ion effects on flows in tokamaks are investigated analytically and numerically. A general analysis of noncollisional electrodynamic momentum transfer from fast ions to bulk plasma is presented, with polarization effects and dissipation in the bulk plasma taken into account. The analysis is illustrated using idealized simulations of fast ion orbits and radial electric fields in the Mega-Ampère Spherical Tokamak (MAST) [A. Sykes, R. J. Akers, L. C. Appel *et al.*, Nucl. Fusion **41**, 1423 (2001)], the Joint European Torus (JET) [P. H. Rebut *et al.*, Nucl. Fusion **25**, 1011 (1985)], and ITER [R. Aymar, P. Barabaschi, and Y. Shimomura, Plasma Phys. Controlled Fusion **44**, 519 (2002)]. In the MAST simulation, prompt losses of beam ions injected counter to the plasma current drive up a radial electric field that saturates at a level such that beam ions subsequently injected are confined electrostatically. Although the actual radial electric fields in counterinjected MAST discharges are lower than this, the scenario explored in the simulation would be approached in MAST plasmas with sufficiently low collisionality. The JET simulation, although unrealistic, shows that a similar process could be driven by losses of fusion α-particles from a burning plasma. Test-particle simulations of α-particles in ITER suggest that performance-limiting instabilities such as neoclassical tearing modes and resistive wall modes could be affected significantly by flows associated with radial fast particle currents. [DOI: 10.1063/1.2801716]

I. INTRODUCTION

Plasma rotation in tokamaks can help to suppress both magnetohydrodynamic (MHD) instabilities, such as sawtooth oscillations,[1] and microinstabilities, such as ion temperature gradient modes, that are believed to cause anomalous transport.[2] For the case of inductive operation in the future burning plasma device ITER,[3] it has recently been calculated that toroidal rotation velocities v_ζ of the order of a few tens of kilometers per second would be sufficient to stabilize neoclassical tearing modes (NTMs) with toroidal and poloidal mode numbers $n=2$, $m=3$,[4] while in the steady-state operation scenario $v_\zeta \simeq 150$ km s^{-1} would be required to suppress the resistive wall mode.[5] It is thus important to be able to predict with confidence the rotation rate in devices such as ITER; to this end it is clearly desirable to understand as fully as possible the mechanisms whereby fast ions can drive this rotation.

Neutral beam injection (NBI) is a well-established method of applying a torque to a tokamak plasma and thereby spinning it toroidally.[6] If injected at sufficiently high energy, the beam ions initially slow down collisionally on electrons and subsequently transfer momentum to bulk ions: the latter process provides a collisional torque to the bulk plasma. An additional torque arises from the fact that the beam ions undergo orbital excursions from the flux surfaces on which they are born.[7] These orbital excursions, in the presence of a radial gradient in the birth profile, give rise to a radial beam ion current that is almost exactly canceled by a return current carried by the bulk ions; the latter produces a $\mathbf{j}\times\mathbf{B}$ torque on the plasma. Experimentally, clear evidence has emerged in recent years that NBI can deliver significant angular momentum to tokamak plasmas via processes that do not involve beam ion collisions. For example, the application of NBI counter to the plasma current direction in the Mega Ampère Spherical Tokamak (MAST) has produced toroidal rotation rates exceeding the local sound speed[8] despite the fact that most of the beam ions are lost from the plasma on time scales of the order of a few tens of microseconds or less; the slowing-down time of beam ions in MAST is around three orders of magnitude longer than this. More recently, toroidal rotation profiles in the DIII-D tokamak have been modified significantly through the use of NBI pulses that are short compared to the beam ion slowing-down time.[9] It has been known for some time that rotation can be produced in tokamaks without the application of a net external torque by heating the plasma using waves in the ion cyclotron range of frequencies (ICRF).[10,11] The fast ions in ICRF-heated plasmas, like those in NBI plasmas, produce radial currents that can drive rotation without the ions being slowed down collisionally.[12]

Helander and co-workers[13] showed that the high rotation rates observed in MAST plasmas with countercurrent NBI could be accounted for by a return current torque of the type discussed in Ref. 7. Also prompted by the MAST countercurrent experiments, McClements and Thyagaraja[14] considered in detail the steady-state return current scenario, in which the Lorentz force due to the radial fast ion current is balanced exactly by viscous forces arising from toroidal momentum relaxation and poloidal flow damping in the

bulk ions, and also a dissipationless insulating scenario, in which the progressive loss of fast ions produces an inward-pointing radial electric field that saturates at a value such that all the fast ions remaining in the plasma are electrostatically confined.

In the present paper, we reconsider the problem of collisionless electrodynamic momentum transfer from fast ions to bulk plasma. In Sec. II, we present a general analysis of the initial value problem, from which the two scenarios considered in Ref. 14 emerge as limiting cases. Bulk ion polarization currents are included in this analysis. In Sec. III, we present results from numerical simulations of collisionless fast ion orbits in MAST, the Joint European Torus (JET), and ITER that provide quantitative estimates of radial currents and the associated electric fields under various conditions in those devices. We present conclusions and discuss some general perspectives suggested by our model in Sec. IV.

II. MODEL

We use a right-handed cylindrical coordinate system (R,ϕ,Z), where R is the distance from the tokamak symmetry axis, ϕ is the toroidal angle, and Z is the vertical distance from the midplane. The plasma equilibrium flux surfaces are labeled by Ψ, which is zero at the magnetic axis and has a positive value on the separatrix, Ψ_s. Thus, $\nabla\Psi$ is directed along the outward normal $\mathbf{n}$ to a flux surface. The poloidal field is given by $\mathbf{B}_\theta=\nabla\times(\Psi\nabla\phi)=\nabla\Psi\times\nabla\phi$, and therefore the plasma current flows in the $-\phi$ direction; the plasma current density j_ϕ is negative. We shall also assume that the toroidal magnetic field B_ϕ is negative. The unit vectors $\mathbf{n}=\nabla\Psi/|\nabla\Psi|$, $\mathbf{e}_\theta=\mathbf{B}_\theta/B_\theta$, $\mathbf{e}_\zeta=-R\nabla\phi$ provide the basis for an alternative right-handed coordinate system: we will refer to this as the (r,θ,ζ) system. We suppose that fast ions are produced in the core region of a quasineutral tokamak plasma in gross mechanical equilibrium with established density and temperature profiles. The fast ions have a birth kinetic energy $\mathcal{E}_f^{\mathrm{in}}$ that is much larger than the bulk ion temperature T_i. Each fast ion has charge Z_fe and mass A_fm_p, where e and m_p are the proton charge and mass. We assume that either bulk ions are removed or electrons are added during this injection process in such a way that overall charge neutrality is never violated.

Since the drifts associated with $\mathbf{E}\times\mathbf{B}$ turbulence are identical for all charged particles, such turbulence cannot drive net radial electric currents, although it can produce radial transport of toroidal momentum, particles, and energy. The radial fast ion current density is typically less than one Am^{-2}.[14] This constitutes a negligible perturbation to the equilibrium tokamak magnetic field, which is produced by currents of typically several MA. For this reason, we shall take the magnetic flux surface geometry to be prescribed. We assume moreover that electrons, by virtue of their small mass, do not carry significant radial currents but short-out significant variations of electrostatic potential Φ on a given flux surface.[14] We thus assume that Φ can be treated as a flux function. Fast ions born with energies much larger than the critical value at which they are coupled equally via collisions to electrons and bulk ions slow down mainly on electrons,[15] which carry negligible momentum in tokamak plasmas. Once the fast ions have slowed down to below their critical energy, they can transfer momentum to the bulk ions via collisions.

We are concerned specifically with electrodynamic effects occurring on time scales that are short compared to the fast particle collision time. First of all, however, it is useful to obtain certain general results concerning the currents in a collisional plasma. We consider a plasma with three species (fast ions, bulk ions, and electrons) that satisfy a system of coupled Fokker-Planck equations. Denoting the distribution function of species j by F_j, the Fokker-Planck equations may be written as follows:

$$\frac{\partial F_f}{\partial t}+\mathbf{v}\cdot\frac{\partial F_f}{\partial \mathbf{r}}+\frac{eZ_f}{m_pA_f}(\mathbf{E}+\mathbf{v}\times\mathbf{B})\cdot\frac{\partial F_f}{\partial \mathbf{v}}=C_{fe}+C_{fi}+C_{ff}+S_f(\mathbf{r},\mathbf{v},t), \tag{1}$$

$$\frac{\partial F_e}{\partial t}+\mathbf{v}\cdot\frac{\partial F_e}{\partial \mathbf{r}}-\frac{e}{m_e}(\mathbf{E}+\mathbf{v}\times\mathbf{B})\cdot\frac{\partial F_e}{\partial \mathbf{v}}=C_{ef}+C_{ei}+C_{ee}+S_e(\mathbf{r},\mathbf{v},t), \tag{2}$$

$$\frac{\partial F_i}{\partial t}+\mathbf{v}\cdot\frac{\partial F_i}{\partial \mathbf{r}}+\frac{eZ_i}{m_pA_i}(\mathbf{E}+\mathbf{v}\times\mathbf{B})\cdot\frac{\partial F_i}{\partial \mathbf{v}}=C_{if}+C_{ie}+C_{ii}+S_i(\mathbf{r},\mathbf{v},t), \tag{3}$$

where the suffixes f, e, and i refer to fast ions, electrons, and bulk ions, respectively, C_{jk} denotes the collision integral for collisions between particles of species j with those of species k, and S_j is the source of particles of species j. The only properties we shall require of the collision integrals are the standard conservation relations of particle number, energy, and momentum consistent with any binary-collision model of the Boltzmann type. The total current density in the system is $\mathbf{j}=\mathbf{j}_f+\mathbf{j}_i+\mathbf{j}_e$, where

$$\mathbf{j}_f=eZ_f\int\mathbf{v}F_fd^3\mathbf{v},$$

$$\mathbf{j}_i=eZ_i\int\mathbf{v}F_id^3\mathbf{v},$$

$$\mathbf{j}_e=-e\int\mathbf{v}F_ed^3\mathbf{v}.$$

In terms of these current densities, the velocity moment equations corresponding to Eqs. (1)–(3) can be written as

$$\mathbf{j}_f\times\mathbf{B}=-eZ_fn_f\mathbf{E}+\mathbf{F}_f^{\mathrm{Ext}}+\mathbf{F}_f^{\mathrm{pol}}+\mathbf{F}_f^{\mathrm{visc}}+\mathbf{F}_{fe}+\mathbf{F}_{fi}, \tag{4}$$

$$\mathbf{j}_i\times\mathbf{B}=-eZ_in_i\mathbf{E}+\mathbf{F}_i^{\mathrm{Ext}}+\mathbf{F}_i^{\mathrm{pol}}+\mathbf{F}_i^{\mathrm{visc}}+\mathbf{F}_{ie}+\mathbf{F}_{if}, \tag{5}$$

$$\mathbf{j}_e\times\mathbf{B}=en_e\mathbf{E}+\mathbf{F}_e^{\mathrm{Ext}}+\mathbf{F}_e^{\mathrm{pol}}+\mathbf{F}_e^{\mathrm{visc}}+\mathbf{F}_{ef}+\mathbf{F}_{ei}. \tag{6}$$

In Eq. (4), $n_f=\int F_fd^3\mathbf{v}$ is the fast ion number density, $\mathbf{E}=-\nabla\Phi=-(\partial\Phi/\partial\Psi)\nabla\Psi$ is the electrostatic field (we neglect the toroidal loop voltage and turbulent electric fields), $\mathbf{F}_f^{\mathrm{Ext}}=\int m_pA_f\mathbf{v}S_fd^3\mathbf{v}$ is the momentum input to the system due to the fast ion source, $\mathbf{F}_f^{\mathrm{pol}}=-m_pA_f\int(\partial F_f/\partial t)\mathbf{v}d^3\mathbf{v}$, $\mathbf{F}_f^{\mathrm{visc}}$

$=-m_p A_f \nabla\cdot(\int F_f \mathbf{v}\mathbf{v} d^3\mathbf{v})$ is a force arising from inertial and viscous stresses, while $\mathbf{F}_{fe}=m_p A_f \int \mathbf{v} C_{fe} d^3\mathbf{v}$ and $\mathbf{F}_{fi}=m_p A_f \int \mathbf{v} C_{fi} d^3\mathbf{v}$ are collisional momentum transfer rates from the fast ions to electrons and bulk ions, respectively. The corresponding quantities in Eqs. (5) and (6) are defined in a similar fashion. The collisional interaction of neutral beam-injected fast ions with bulk ions is considered in detail in Ref. 16.

We are concerned with the currents that flow perpendicular to the magnetic flux surfaces Ψ. Taking the cross product of Eq. (4) with $\mathbf{B}$ and dividing by B^2, we obtain

$$\mathbf{j}_{\perp f}=\frac{\mathbf{B}\times(-eZ_f n_f \mathbf{E}+\mathbf{F}_f^{\mathrm{Ext}}+\mathbf{F}_f^{\mathrm{pol}}+\mathbf{F}_f^{\mathrm{visc}}+\mathbf{F}_{fe}+\mathbf{F}_{fi})}{B^2}.$$

Similar expressions can be obtained for $\mathbf{j}_{\perp i,e}$. Having computed the local perpendicular fast ion current density, we can then obtain the average current density flowing through the flux surface:

$$j_f^{\Psi}=\frac{\oint_{\Psi}(\mathbf{j}_{\perp f}\cdot\mathbf{n})2\pi R dl}{\oint_{\Psi}2\pi R dl}, \tag{7}$$

where dl is an arc length along the flux surface in the poloidal plane. We may write

$$j_f^{\Psi}=j_f^{*}+j_f^{i}+j_f^{e}, \tag{8}$$

where

$$j_f^{*}=\oint_{\Psi}(\mathbf{n}\times\mathbf{B})\cdot\frac{(\mathbf{F}_f^{\mathrm{Ext}}+\mathbf{F}_f^{\mathrm{pol}}+\mathbf{F}_f^{\mathrm{visc}})}{B}\frac{dA}{A(\Psi)}, \tag{9}$$

$$j_f^{i}=\oint_{\Psi}(\mathbf{n}\times\mathbf{B})\cdot\frac{\mathbf{F}_{fi}}{B}\frac{dA}{A(\Psi)}, \tag{10}$$

$$j_f^{e}=\oint_{\Psi}(\mathbf{n}\times\mathbf{B})\cdot\frac{\mathbf{F}_{fe}}{B}\frac{dA}{A(\Psi)}. \tag{11}$$

Here $\mathbf{b}=\mathbf{B}/B$ is the unit tangent vector to a field line ($\mathbf{n}\cdot\mathbf{b}=0$), $A(\Psi)$ is the total area of flux surface Ψ, and $dA=2\pi R dl$. The electric field term in Eq. (4) does not contribute to j_f^{*} since the electrostatic potential is taken to be a flux function. We can obtain similar expressions for the currents j_i^{Ψ} and j_e^{Ψ} using the corresponding moment equations.

Whereas j_f^{*} is intrinsic to the fast ions, being determined by the source, inertia, and self-collisions of those particles, j_f^{i} and j_f^{e} are due to collisional momentum exchange between the fast ions and the bulk plasma. Since all binary Coulomb collisions conserve momentum, it follows that $j_f^{i}+j_i^{f}=0$, $j_f^{e}+j_e^{f}=0$, and $j_i^{e}+j_e^{i}=0$, where j_i^{f}, j_e^{f}, j_i^{e}, and j_e^{i} are given by expressions analogous to those in Eqs. (10) and (11). As a result of these cancellations, the total flux surface-averaged current density is

$$\begin{aligned} j_{\mathrm{tot}}^{\Psi}&=(j_f^{*}+j_f^{i}+j_f^{e})+(j_e^{*}+j_e^{i}+j_e^{f})+(j_i^{*}+j_i^{f}+j_i^{e}),\\ &=j_f^{*}+j_i^{*}+j_e^{*}. \end{aligned} \tag{12}$$

Taking the surface integral of Ampère's law over flux surface Ψ, we thus obtain

$$j_f^{*}+j_i^{*}+j_e^{*}=\epsilon_0\frac{\partial}{\partial t}\left(\frac{\partial\Phi}{\partial\Psi}\oint_{\Psi}|\nabla\Psi|\frac{dA}{A}\right), \tag{13}$$

where ϵ_0 is the permittivity of free space. This equation is exact if turbulence is negligible, the magnetic field is constant, and the electrostatic potential is a flux function. In general, the currents on the left-hand side involve both Φ and its time derivative: they are functionals of the electric and magnetic fields both directly and via the distribution functions $F_{f,e,i}$. Under standard tokamak conditions j_e^{*} can be neglected;[14] we will show later that the vacuum displacement current [the term on the right-hand side of Eq. (13)] is also very small. The evolution equation for $\Phi(\Psi,t)$ then has the relatively simple form

$$j_f^{*}(\Psi,t,\Phi,\partial\Phi/\partial t;F_f)=-j_i^{*}(\Psi,t,\Phi,\partial\Phi/\partial t;F_i). \tag{14}$$

It should be noted that this is actually a differential equation for Φ as a function of Ψ,t, which must be solved simultaneously with the Vlasov equations for F_f and F_i given the magnetic geometry, $\mathbf{E}=-(\partial\Phi/\partial\Psi)\nabla\Psi$, the sources and the plasma profiles. Physically, it states that the fast ions, by virtue of their sources and energy, produce a radial current as they move in the self-consistent electric field. To preserve local quasineutrality within each flux surface, the fast ion current must be balanced exactly by a bulk ion return current driven purely by self-collisions and reactive effects (rather than frictional currents between species).

On time scales that are short compared to the slowing-down time, the fast ions can be regarded as collisionless and Eq. (1) reduces to

$$\frac{\partial F_f}{\partial t}+\mathbf{v}\cdot\frac{\partial F_f}{\partial\mathbf{r}}+\frac{eZ_f}{m_p A_f}(\mathbf{E}+\mathbf{v}\times\mathbf{B})\cdot\frac{\partial F_f}{\partial\mathbf{v}}=S_f(\mathbf{r},\mathbf{v},t), \tag{15}$$

where the source S_f depends on the bulk plasma parameters and the method of injection. In the case of ICRF heating, the resonant ions will be heated locally to high temperatures at some rate fixed by the antenna power and other plasma characteristics. In the case of D-T fusion reactions, the bulk D and T ions will be transformed into α-particles with energies around 3.5 MeV, approximately isotropic in velocity space but rather strongly localized to the core, depending upon the pressure profile $p(\Psi)$ (in the temperature range relevant to tokamak burning plasmas, the reaction rate scales approximately as p^2). In the case of NBI, the injected atoms are ionized by bulk ions or electrons (usually the former). Even before fast ion injection starts, there will be an electric field in the tokamak due to the bulk plasma pressure gradient and other effects. However, this can be neglected whenever the injected fast ion energies are much higher than the electron and ion temperatures.

It is not necessary to solve Eq. (15) to gain a qualitative understanding of the nature and characteristics of the intrinsic fast ion current j_f^{*}. Consider N_f fast ions with initial ki-

netic energy $\mathcal{E}_f^{\text{in}}$ and their associated electrons introduced instantaneously on a particular flux surface Ψ_0. We assume that all the fast ions are confined by the poloidal magnetic field and, to begin with, we neglect the bulk plasma. The electrons are restricted to the neighborhood of Ψ_0 due to their negligible mass. The fast ions, on the other hand, undergo significant radial displacements both inwards and outwards. An electric polarization $\mathbf{P}(\Psi,t)$ is produced by these particles, with the main contribution coming from the trapped population: the polarization extends over a radial distance of the order of the trapped fast ion orbit width. The polarization implies a net positive charge density both within Ψ_0 and outside it, with a strong negative charge density in its vicinity. The net charge enclosed by flux surface Ψ, which is given by $Q(\Psi)=-\oint_\Psi \mathbf{P}\cdot\mathbf{n}dA$, is positive for $0<\Psi<\Psi_0$ and negative for $\Psi_0<\Psi<\Psi_{\max}$, tending to zero at the last closed flux surface $\Psi_{\max}$. The electric displacement takes place over a period of the order of a few trapped particle bounce times. The fast ion current density is equal to $\partial\mathbf{P}/\partial t$; the flux surface-averaged radial component of this is negative within Ψ_0 and positive outside Ψ_0. The fast ions are rapidly redistributed, losing some fraction of their initial kinetic energy to the electrostatic field in the process.

The polarization produced by displacements of the fast ions tends to a steady value determined by the initial state of those ions: the fast ion current must therefore decay to zero. Since, in this scenario, there is no bulk plasma, the total initial fast ion energy must equal the fast ion kinetic energy plus the electrostatic field energy at later times (electrons are taken to have negligible mass and are assumed to be cold). Similarly, the initial fast ion toroidal angular momentum must equal the angular momentum of the fast ions plus that of the field at later times. This result is proven in the Appendix.

If a collisionless bulk plasma is introduced into the above scenario, the fast ions still produce an electric polarization, since they cannot be influenced directly by the bulk ions in the absence of collisions. However, the changing electric field this creates causes the bulk ions to shield the negative charge density trough developing at Ψ_0. In other words, the bulk ions move in response to their inertial/polarization current and reduce the negative charge density at Ψ_0 and the net positive charge densities on either side relative to the vacuum scenario. This implies that j_f^* is partly canceled by j_i^*, and that the electric field rises more slowly than in the vacuum case. It can be shown that almost all of the energy and toroidal angular momentum of the injected fast ions is transferred into the bulk ions rather than into the field.

If there is an extended series of similar injections, each set of N_f injected fast ions contributes to j_f^* as the polarization they create is established dynamically. So long as new fast ions are injected at a fixed rate, the collisionless torque on the bulk ions can be maintained. Most of this torque is provided by the trapped fast ions. If the source distribution is inhomogeneous, it is clear that the fast ions can deliver momentum to the bulk plasma as they create net polarization. In the absence of collisions, the plasma must continue to spin up under this continuous electrodynamic conversion of injected momentum. The precessional toroidal momentum of trapped fast ions is generally much lower than their toroidal momentum at birth. Passing fast ions can transfer some of their momentum to the field because their drift orbits deviate from the flux surface of birth, but the contribution of these ions to the torque is smaller than that made by trapped fast ions by a factor of the order of the square root of the local inverse aspect ratio. In Sec. III, exact orbit calculations will be used to show that this qualitative description is correct. In the presence of bulk plasma dissipation, a steady state can result either from a balance between the collisionless input torque and bulk plasma momentum losses (both neoclassical and turbulent) or through the creation of an electric field that is large enough to prevent fast ion polarization.

The fast ion current is a function of the radial electric field since the former is determined by the characteristic equations of the Vlasov equation [Eq. (15)], i.e., the Lorentz force equation. According to this equation, toroidal canonical momentum $p_\phi=A_f m_p R v_\phi+Z_f e\Psi$ is a constant of the motion if the fields are axisymmetric, while the temporal evolution of total particle energy $\mathcal{E}_T$ (kinetic plus potential) is described by

$$\frac{d\mathcal{E}_T}{dt}=Z_f e\frac{\partial\Phi}{\partial t}, \tag{16}$$

where the time derivative of Φ is evaluated at the instantaneous particle position. Monte Carlo particle simulations, presented in Sec. III, generally indicate that Φ decreases monotonically on every flux surface. Thus, particle energies must decrease in time and none of the fast ions can leave the birth region if the magnitude of the radial electric field is sufficiently large.

We now return to Eq. (13), retaining for the moment the displacement current term on the right-hand side but neglecting the electron term on the left-hand side. As indicated previously, the fast ion current j_f^* is a functional of the fast ion source S_f in Eq. (15), the equilibrium magnetic field, and the electric field. It can be computed numerically by solving Eq. (15) provided that $\Phi(\Psi,t)$ is known. Following Ref. 14, we can estimate j_i^*, the bulk ion term in Eq. (13), as follows. We first note that Eq. (13) can be written in the form

$$j_f^*+j_r+\epsilon_0\frac{\partial E}{\partial t}=0, \tag{17}$$

where E is the flux surface-averaged radial electric field and $j_r\equiv j_i^*$ is the flux surface-averaged bulk ion return current density. Denoting by v_r, v_θ, and $v_\zeta=-v_\phi$ the flux surface-averaged radial, poloidal, and toroidal bulk ion fluid velocity components, neglecting pressure gradient and $(\mathbf{v}\cdot\nabla)\mathbf{v}$ terms, and taking the limit of large aspect ratio, we can write the bulk ion equations of motion in the (r,θ,ζ) system as

$$\left(\frac{A_i m_p}{Z_i e}\right)\frac{\partial v_r}{\partial t}=E+v_\theta B_\zeta-v_\zeta B_\theta, \tag{18}$$

$$\rho_m\frac{\partial v_\theta}{\partial t}=-j_r B_\zeta-\rho_m\nu_\theta v_\theta, \tag{19}$$

$$\rho_m \frac{\partial v_\zeta}{\partial t} = j_r B_\theta - \rho_m \nu_\zeta v_\zeta, \tag{20}$$

where ρ_m is the bulk ion mass density, and ν_θ and ν_ζ are poloidal and toroidal momentum relaxation rates. In these equations, B_ζ is the toroidal field at the magnetic axis; in the assumed large aspect ratio limit, the poloidal field B_θ is constant on a flux surface. The large aspect ratio approximation is of course more accurate for JET and ITER than it is for a spherical tokamak such as MAST, but the equations provide a useful qualitative description of the response of the bulk ion fluid to the presence of a fast ion radial current even in a tight aspect ratio device.[14] It is reasonable to neglect the pressure gradient term in Eq. (18) in the case of MAST discharges with countercurrent beam injection, since the flow-induced contribution to the radial electric field is typically around 40 times larger than the pressure gradient contribution.[14]

We shall verify *a posteriori* that in Eq. (18) the inertia term is negligible and write the equation in the form

$$E = -v_\theta B_\zeta + v_\zeta B_\theta. \tag{21}$$

In the case of the poloidal flow, damping occurs because of an effective friction between trapped and passing ions. Neoclassical calculations indicate that the damping is not strictly exponential[17,18] but the overall decay is characterized by a rate given by $\nu_\theta \simeq (2R/3r)\nu_{ii}$ (Ref. 18), where ν_{ii} is the ion-ion collision rate. For the toroidal flow, the relaxation rate is much lower and is generally determined by turbulent processes rather than collisions. According to neoclassical theory, the radial diffusivity of toroidal flow in the banana regime is $\chi_\zeta \simeq (1/10)q^2\rho_i^2\nu_{ii}$, where q is the tokamak safety factor and ρ_{*i} is the bulk ion Larmor radius;[19] this result implies that $\nu_\zeta \simeq (1/10)q^2\rho_{*i}^2\nu_{ii}$, where $\rho_{*i}=\rho_i/a$, a being the plasma minor radius. As noted in Ref. 9, experimentally determined values of ν_ζ are generally much higher than this.

A. Solutions in the dissipationless limit

Before considering the general problem of relating j_r to E, it is instructive to consider the strictly dissipationless case with $\nu_\theta = \nu_\zeta = 0$. Differentiating Eq. (21) with respect to t and substituting from Eqs. (19) and (20), we obtain

$$j_r = \frac{\rho_m}{B^2}\frac{\partial E}{\partial t}. \tag{22}$$

Thus, in the absence of dissipation, the return current is equal to the polarization current, and as such it depends on the time derivative of the electric field rather than the electric field itself. The scaling with ρ_m in this result shows that electrons make a negligible contribution to j_r. Using Eq. (22) to eliminate j_r from Eq. (17), we obtain an evolution equation for the electric field,

$$j_f^* + \epsilon_0\left(1 + \frac{c^2}{c_A^2}\right)\frac{\partial E}{\partial t} = 0, \tag{23}$$

where c is the speed of light, $c_A \equiv B/(\mu_0\rho_m)^{1/2}$ is the Alfvén speed, and $j_f^* = |\mathbf{j}_f|$. In this limit, the plasma behaves like a dielectric with permittivity,

$$\epsilon = \epsilon_0\left(1 + \frac{c^2}{c_A^2}\right). \tag{24}$$

Thus, for a given $j_f^* > 0$, the radial electric field evolves much more slowly in a plasma than it would in a vacuum whenever $c_A \ll c$, which is invariably the case in tokamaks. Under typical conditions, the rate of change of the electric field lies well below the characteristic frequency of geodesic acoustic modes (GAMs) v_i/R, where v_i is the bulk ion thermal speed,[20] and therefore such modes cannot be excited in the absence of turbulence.[21] It should be noted that in this dissipationless limit, it is not necessary to distinguish between trapped and passing bulk ions since all of these ions are subject to the same polarization drift and thus contribute equally to the return current. The relevant time scales in this regime are short compared to the bulk ion self-collision time, and therefore results from neoclassical theory[22,23] are not applicable.

Equation (23) can be solved simultaneously with the fast ion Vlasov equation [Eq. (15)] for a given magnetic equilibrium and fast particle source to determine the temporal evolution of the radial electric field and fast ion current in the dissipationless limit. Because the electric field changes relatively slowly, the bulk plasma return current almost exactly cancels the fast ion current at each instant until $j_f^* = 0$. The qualitative behavior of j_f^* as a function of E can be readily understood. As the fast ions move out from their birth region, the negative charge density rises and consequently the inward-pointing electric field also rises. This field draws in bulk ions that partly cancel the space charge: this slows down the rise of the inward-pointing field but does not stop it completely. As the field evolves, the fast ion current normal to a given flux surface decreases monotonically, becoming negligibly small for some electric field $E = E^{\mathrm{crit}}(r) < 0$. The existence of such a field arises from the fact that total particle energy $\mathcal{E}_T$ is an approximate constant of the motion, since on any given flux surface Φ evolves only slowly with time [cf. Eq. (16)]. If $|E|$ is sufficiently large, $\mathcal{E}_T \simeq Z_f e\Phi$, and since $\Phi = \Phi(\Psi)$ it follows that the particle drift orbit lies on a flux surface and the particle therefore no longer produces an electric polarization. Roughly, we may expect $|E^{\mathrm{crit}}|$ to be of the order of $\mathcal{E}_f^{\mathrm{in}}/(eZ_f)$ divided by the orbit width in the absence of the electric field.

With these considerations in mind, we consider a simple model in which j_f^* depends linearly on E,

$$\begin{aligned} j_f^* &= K\dot{N}_f(E - E^{\mathrm{crit}})H(E - E^{\mathrm{crit}}), \\ &= j_f^*(0)\left[1 - \frac{E}{E^{\mathrm{crit}}}\right]H(E - E^{\mathrm{crit}}), \end{aligned} \tag{25}$$

where K is a constant for a given flux surface, $j_f(0) = -K\dot{N}_f E^{\mathrm{crit}}$ is the fast ion current when $E=0$, and the Heaviside function $H(x)$ is equal to 1 for $x>0$ and vanishes for $x \le 0$. In principle, K and E^{crit} can vary with Ψ (or, equivalently, with r). They can be determined by solving Eq. (15) for a given S_f and a fixed $\Phi(\Psi)$. Substituting Eq. (25) in Eq. (23), we obtain

$$\frac{\partial}{\partial t}\left(\frac{E}{E^{\mathrm{crit}}}\right)=\frac{j_f^*(0)}{|E^{\mathrm{crit}}|\epsilon_0(1+c^2/c_A^2)}\left(1-\frac{E}{E^{\mathrm{crit}}}\right),$$

$$=-\lambda_f\left(\frac{E}{E^{\mathrm{crit}}}-1\right), \tag{26}$$

where $\lambda_f=j_f^*(0)/|E^{\mathrm{crit}}|\epsilon_0(1+c^2/c_A^2)$. In this model, E/E^{crit} increases monotonically from zero to unity in a characteristic time $1/\lambda_f$ and the field equals E^{crit} when the fast ion current density reaches zero. With $E=0$ at $t=0$, Eq. (26) has the solution

$$E=E^{\mathrm{crit}}[1-\exp(-\lambda_f t)]. \tag{27}$$

Substituting this result in Eq. (25), we obtain

$$j_f^*=j_f^*(0)\exp(-\lambda_f t). \tag{28}$$

One can use this solution to verify that for typical fast particle production rates, the neglect of the inertia term in Eq. (18) is fully justified. Consider, for example, fusion α-particles in JET ($c_A\sim 10^7$ ms^{-1}) with $j_f^*(0)<1$ Am^{-2} and $E^{\mathrm{crit}}>1$ MVm^{-1}. For these parameters, $\lambda_f^{-1}>10$ ms: identifying this as the characteristic time scale on which v_r evolves, we find that the inertia term in Eq. (18) is smaller than the other terms by many orders of magnitude.

B. Solutions with bulk ion dissipation

We now present a simplified analysis in which bulk ion momentum relaxation is retained but we neglect the inertia term in Eq. (18) and assume exact cancellation of the fast ion current and the return current. Equation (24) shows that in the collisionless limit, the return polarization current exceeds the displacement current by a factor of c^2/c_A^2, which is around 10^3 in JET. The contribution of the displacement current to the radial component of Ampère's law remains small in the collisional case. With the inertia term in Eq. (18) dropped and $j_r=-j_f^*=-K\dot{N}_f(E-E^{\mathrm{crit}})=-j_f^*(0)(1-E/E^{\mathrm{crit}})$ for $E^{\mathrm{crit}}\le E\le 0$, Eqs. (18)–(20) can be solved exactly. We consider first the steady limit in which the equations reduce to the inhomogeneous linear system,

$$E+v_\theta B_\zeta-v_\zeta B_\theta=0, \tag{29}$$

$$j_f^*(0)\left(\frac{E}{E^{\mathrm{crit}}}\right)B_\zeta+\rho_m\nu_\theta v_\theta=j_f^*(0)B_\zeta, \tag{30}$$

$$-j_f^*(0)\left(\frac{E}{E^{\mathrm{crit}}}\right)B_\theta+\rho_m\nu_\zeta v_\zeta=-j_f^*(0)B_\theta. \tag{31}$$

Equations (30) and (31) can be used to eliminate v_θ and v_ζ from the first equation, leading to the following expression for E/E^{crit}:

$$\left(\frac{E}{E^{\mathrm{crit}}}\right)=\frac{\mu_0 j_f^*(0)\left(\frac{c_{A\zeta}^2}{\nu_\theta}+\frac{c_{A\theta}^2}{\nu_\zeta}\right)}{\mu_0 j_f^*(0)\left(\frac{c_{A\zeta}^2}{\nu_\theta}+\frac{c_{A\theta}^2}{\nu_\zeta}\right)+|E^{\mathrm{crit}}|}, \tag{32}$$

where $c_{A\zeta}^2=B_\zeta^2/\mu_0\rho_m$ and $c_{A\theta}^2=B_\theta^2/\mu_0\rho_m$. Putting this expression into Eqs. (30) and (31), we obtain

$$v_\theta=\left(\frac{j_f^*(0)B_\zeta}{\rho_m\nu_\theta}\right)\left(1-\frac{E}{E^{\mathrm{crit}}}\right), \tag{33}$$

$$v_\zeta=-\left(\frac{j_f^*(0)B_\theta}{\rho_m\nu_\zeta}\right)\left(1-\frac{E}{E^{\mathrm{crit}}}\right). \tag{34}$$

It should be noted here that $j_f^*(0)$ is the nonambipolar component of the fast ion current density at a given radius r in the absence of a radial electric field. It depends only upon the magnetic geometry and the source profile and birth energy of the fast ions, as does E^{crit}. Since $B_\theta>0$, it follows from Eq. (33) that $v_\zeta<0$. Since $j_\zeta>0$, the driven toroidal flow is in the countercurrent direction. Neoclassical theory can be used to infer a poloidal flow velocity that depends on the ion temperature gradient:[22] this cannot be recovered from Eq. (33) in the absence of fast ions $[j_f^*(0)\to 0]$ since, as discussed previously, pressure gradients have been neglected in the radial component of the bulk ion momentum equation.

Equation (32) shows that $|E|\le|E^{\mathrm{crit}}|$ on any given flux surface. It follows from this equation that if the fast ion source parameters are such that

$$\mu_0 j_f^*(0)\left(\frac{c_{A\zeta}^2}{\nu_\theta}+\frac{c_{A\theta}^2}{\nu_\zeta}\right)\ll|E^{\mathrm{crit}}|,$$

then [cf. Eq. (9) of Ref. 14]

$$E\simeq-\mu_0 j_f^*(0)\left(\frac{c_{A\zeta}^2}{\nu_\theta}+\frac{c_{A\theta}^2}{\nu_\zeta}\right). \tag{35}$$

This is the steady-state radial electric field in the limit of low fast particle production rates, low fields, or high collisionality: E is much smaller than the critical value required to quench the fast ion current flowing across that flux surface. In deriving this result, we have assumed that the bulk ion flows can be described in terms of simple relaxation rates and are not dependent on flow gradients. If strong flow gradients are present, it would be necessary to solve radial differential equations to obtain the flows.

When the fast particle production rate or magnetic field are sufficiently high, or the collisionality is sufficiently low, the above inequality is reversed and we obtain from Eq. (32) the result

$$E\simeq E^{\mathrm{crit}}. \tag{36}$$

In this case, bulk ion return currents play no role in determining the radial electric field. From Eqs. (33) and (34), we see generally that in steady state [cf. Eq. (11) in Ref. 14]

$$\frac{v_\theta}{v_\zeta}=-\frac{B_\zeta\nu_\zeta}{B_\theta\nu_\theta}. \tag{37}$$

Combining this relation with Eqs. (29) and (36), we find that

$$v_\zeta\simeq\left(\frac{E^{\mathrm{crit}}}{B_\theta}\right)\left(1+\frac{\nu_\zeta B_\zeta^2}{\nu_\theta B_\theta^2}\right)^{-1}. \tag{38}$$

The maximum toroidal rotation rate $v_\zeta=E^{\mathrm{crit}}/B_\theta$ thus occurs when, in addition to

$$\mu_0 j_f^*(0)\left(\frac{c_{A\zeta}^2}{\nu_\theta}+\frac{c_{A\theta}^2}{\nu_\zeta}\right) \gg |E^{\rm crit}|, \tag{39}$$

the following inequality is satisfied:

$$\left(\frac{B_\zeta}{B_\theta}\right)^2 \ll \frac{2R}{3r}\nu_{ii}\tau_\zeta, \tag{40}$$

where we have assumed that $\nu_\theta \simeq (2R/3r)\nu_{ii}$, in accordance with neoclassical theory,[18] and $\tau_\zeta = 1/\nu_\zeta$ is the toroidal momentum confinement time: this is generally found to be of the order of the energy confinement time τ_E (cf. Refs. 9 and 14). Since q is approximately equal to $(r/R)B_\zeta/B_\theta$, Eq. (40) can be rewritten in the form

$$\left|\frac{B_\zeta}{B_\theta}\right| \ll \frac{2}{3q}\nu_{ii}\tau_\zeta. \tag{41}$$

In spherical tokamaks such as MAST, Eq. (41) is easily satisfied, since $q \sim 1$, $B_\theta \sim B_\zeta$, while the energy confinement time is much longer than $1/\nu_{ii}$. In high-performance JET plasmas, with densities of a few times 10^{19} m^{-3} and ion temperatures of around 10 keV, the ion-ion collision time is of the order of 50 ms while the energy confinement time is typically a few hundred ms. With $q \sim 1$ and $B_\zeta/B_\theta \sim R/r \geq 3$, we find that the quantities on the left- and right-hand sides of Eq. (41) are typically of the same order of magnitude under JET conditions. In ITER, τ_E and hence τ_ζ are predicted to be a factor of 10 or more higher than in JET while ν_{ii}, q, and B_ζ/B_θ have roughly the same values, so that Eq. (41) should be easily satisfied, as in spherical tokamaks. The maximum rotation rate will only be realized, however, if Eq. (39) is also satisfied. We will discuss this issue in Sec. III in light of numerical computations of $j_f^*(0)$.

It is important to note that when Eq. (36) is satisfied, the mechanical toroidal angular momentum acquired by the bulk plasma does not depend on the fast ion current. Moreover, fast ions born at sufficiently high energy collide mainly with electrons, and do not deposit significant momentum via collisions to the bulk ions. The passing fast ions can deposit momentum to the bulk ions by collisions when they have slowed down below the critical energy. Momentum conservation requires that the radial currents in the two species due to such friction forces be equal and opposite. However, the radial electric field produced by the fast ion current does work on the bulk ions carrying the return current: the power density delivered to the bulk ions is simply Ej_f^*.

We now address the problem of solving the full time-dependent bulk ion equations of motion with $j_f^* = -j_r$ given by Eq. (25). The steady scenario considered above has yielded a particular integral of these equations; the appropriate complementary function can be obtained by solving the homogeneous time-dependent system

$$E = -v_\theta B_\zeta + v_\zeta B_\theta, \tag{42}$$

$$\rho_m \frac{\partial v_\theta}{\partial t} = -j_f^*(0)\left(\frac{E}{E^{\rm crit}}\right)B_\zeta - \rho_m \nu_\theta v_\theta, \tag{43}$$

$$\rho_m \frac{\partial v_\zeta}{\partial t} = j_f^*(0)\left(\frac{E}{E^{\rm crit}}\right)B_\theta - \rho_m \nu_\zeta v_\zeta. \tag{44}$$

Setting $E/E^{\rm crit} = xe^{-\lambda t}$, $v_\theta = y(E^{\rm crit}/B_\zeta)e^{-\lambda t}$, and $v_\zeta = z(E^{\rm crit}/B_\theta)e^{-\lambda t}$, where x, y, and z are dimensionless time-independent quantities, we find that they and the decay parameter λ satisfy the set of equations

$$x + y - z = 0,$$

$$j_f^*(0)B_\zeta x - \rho_m(\lambda - \nu_\theta)y\frac{E^{\rm crit}}{B_\zeta} = 0,$$

$$-j_f^*(0)B_\theta x - \rho_m(\lambda - \nu_\zeta)z\frac{E^{\rm crit}}{B_\theta} = 0.$$

Setting the determinant of coefficients of x, y, and z equal to zero yields a quadratic equation for the decay rate eigenvalues λ, with solutions

$$2\lambda = \nu_\theta + \nu_\zeta + \frac{\mu_0 j_f^*(0)c_A^2}{|E^{\rm crit}|} \pm \sqrt{\left\{\nu_\theta + \nu_\zeta + \frac{\mu_0 j_f^*(0)c_A^2}{|E^{\rm crit}|}\right\}^2 - 4\nu_\theta\nu_\zeta\left\{1 + \frac{\mu_0 j_f^*(0)\left(\frac{c_{A\theta}^2}{\nu_\zeta}+\frac{c_{A\zeta}^2}{\nu_\theta}\right)}{|E^{\rm crit}|}\right\}}. \tag{45}$$

The general solution for the flow and the radial electric field is the sum of the steady solution of the inhomogeneous system found previously and a complementary function comprising two eigenmodes corresponding to the above eigenvalues, with arbitrary constants fixed by the initial conditions. It is usually the case that $\nu_\theta \gg \nu_\zeta$. If in addition the collisionality is sufficiently low that $\nu_\theta \ll \mu_0 j_f^*(0)c_A^2/|E^{\rm crit}|$, one of the eigenvalues reduces to the collisionless value λ_f discussed previously. If, on the other hand, $\mu_0 j_f^*(0)c_A^2/|E^{\rm crit}| \ll \nu_\theta$, ν_ζ, the two eigenvalues are approximately equal to ν_θ and ν_ζ. The toroidal flow will reach its steady value, given by Eq. (34), on the relatively long time scale $1/\nu_\zeta$. It should be noted that the function j_f^* is constrained only by the requirements that it should increase monotonically with E in the interval $-|E^{\rm crit}| < E \leq 0$ and vanish for $E < -|E^{\rm crit}|$: thus, many solutions other than those discussed above are possible. For any specified $j_f^*(E)$ one can in principle find both the steady solution and the temporal evolution of E on each flux surface, given values of the parameters ρ_m, ν_θ, and ν_ζ characterizing the bulk ions. In general,

however, the equations depend nonlinearly on E and must be solved numerically.

Many tokamak plasmas have significant concentrations of impurity ions with $Z_i \gg 1$, $A_i \gg 1$. The inertial response of the plasma to a fast particle radial current will be determined by the mass density of all the ion species: a very massive minority ion species could contribute significantly to ρ_m and hence the return current despite having a relatively low number density. A rise in ρ_m would imply an increase in the ratio c^2/c_A^2 and hence slow down the rise in the radial electric field [cf. Eq. (10)]. This predicted slowing down could in principle be measured by injecting very high mass impurity ions in discharges with pulsed NBI, such as those discussed by deGrassie and co-workers.[9] The cylindrical plasma model can be extended in a straightforward way to take into account the effects of impurities by considering the momentum balance equations for the impurity species, incorporating their collisional interactions with the bulk ions. The fast ion current will then be balanced by the sum of the return currents of the bulk and impurity ions. The analysis is similar to that presented in the pure plasma case; the results will be affected by the presence of impurities but the qualitative trends will be the same as those found before. Impurities often provide excellent diagnostic tools for the measurement of flows, and it may be worthwhile to consider particular minority ion scenarios in order to subject the model to systematic experimental checks.

It was noted earlier that sufficiently energetic fast particles slow down primarily on electrons. This momentum-conserving process leads to an exact cancellation of the resultant radial currents in the fast ions and the electrons: the net particle transport is ambipolar. The fast ions heat the electrons but do not transfer significant momentum; the plasma in fact loses momentum as the fast ions are transported out of the system. There is, however, a process whereby electrons themselves can give rise to an intrinsic radial current that could drive a bulk ion return current. Static magnetic perturbations that destroy the flux surfaces of an axisymmetric tokamak field can give rise to a stochastic radial electron diffusivity $D \simeq v_e q R (\delta B/B)^2$, where v_e is the electron thermal speed, R is major radius, and $\delta B/B$ is the relative amplitude of the perturbation.[24] For the case of 10 keV electrons in JET ($R \simeq 3$ m), the diffusivity corresponding to $\delta B/B \simeq 10^{-4}$, a typical perturbation amplitude, is around 1 $m^2\ s^{-1}$. For typical values of the electron density n_e in JET, this would generate a radial electron current $j_e^* \simeq -eD|\nabla n_e| \simeq 1\ \mathrm{Am}^{-2}$. Since, by virtue of their large mass, the bulk ions are not transported significantly by magnetic turbulence, momentum balance under these circumstances requires the generation via polarization and dissipative effects of a bulk ion return current j_i^* and a radial electric field, as discussed in the fast ion case. This mechanism can also operate when electrons are lost rapidly from the system due to MHD instabilities. The bulk ions respond in a similar fashion to intrinsic radial currents carried by electrons and fast ions, except that the direction of the bulk ion return current is different in the two cases if the fast ion/electron particle fluxes are radially outward.

We consider finally the possible effects of turbulence on the fast ions. Trapped fast ions close to their bounce points move relatively slowly and could thus be scattered by long parallel wavelength modes, with an effective collision time τ that depends on the turbulence decorrelation time scale (this is of the order of the linear growth times of many common instabilities). Moreover, passing fast ions close to the trapped/passing boundary are vulnerable to being scattered into trapped orbits due to the presence of turbulence. Taking the effective step length Δ to be the fast ion orbit width, and the collision time to be determined by the turbulence time scale, we find that the corresponding diffusivity $D = \Delta^2/\tau$ can easily be of the order of 1 $m^2\ s^{-1}$. This would be sufficient to produce a significant nonambipolar fast ion current j_f^*. Once again, this anomalous fast particle current could drive up a substantial radial electric field and associated rotation. Since the fast ion current is collisionless, it could be computed by solving Eq. (15) for fast ions in a tokamak plasma with a prescribed turbulent spectrum of **E** and **B** fields. In future work, we intend to investigate fast particle transport and associated electric field effects in the presence of tokamak turbulence. Such an investigation should take into account *inter alia* the effects of GAMs, which can be excited by turbulent electric fields in toroidal geometry.[20]

III. SIMULATIONS

In this section, we present results from numerical calculations of the radial currents due to fast particles in MAST, JET, and ITER-like plasmas. The code TOPAS[25] is used to solve simultaneously the full orbit equations of collisionless fast ions and the flux surface-averaged form of Poisson's equation [equivalently, the flux surface-averaged form of Ampère's law, Eq. (13)], with the space charge in the latter determined by orbital excursions of the fast ions from flux surfaces. In the case of the MAST simulation, the code includes bulk ion dynamics via the collisionless return current term in Eq. (13), as well as the displacement current term. As noted in Sec. II, the polarization return current exceeds the displacement current by a factor of c^2/c_A^2, but both are proportional to $\partial E/\partial t$, the total permittivity being given by Eq. (24). This contrasts with the value derived in Ref. 23,

$$\epsilon = \epsilon_0 \left(1 + \frac{c^2}{c_{A\theta}^2} \right), \tag{46}$$

which is appropriate for time scales longer than a poloidal damping time $(1/\nu_\theta)$ after the start of fast ion injection. On such time scales, the poloidal flow saturates due to neoclassical damping, and is much smaller than the poloidal component of the $\mathbf{E} \times \mathbf{B}$ guiding center drift velocity. If the radial electric field is sufficiently large that the bulk ion pressure gradient makes a negligible contribution to radial momentum balance, the toroidal flow is then given in terms of E by the ideal MHD relation,

$$v_\zeta = E/B_\theta. \tag{47}$$

These circumstances do not apply during the initial growth of the electric field, which is a nearly collisionless process. In this section, we are concerned with the (collisionless) insulating scenario in which the classical permittivity given by

Eq. (24) is appropriate. This is also for practical convenience: it would take a prohibitively long time to simulate a sufficiently large number of particles for E to be calculated accurately over the tens of milliseconds expected to be required under MAST conditions for a steady state to be reached using the neoclassical permittivity.

In TOPAS, Poisson's equation is solved for the electrostatic potential Φ as a function of poloidal flux Ψ and time in a volume-integrated form, with the total net charge within the volume enclosed by the flux surface Ψ being evaluated at each time step. The computed radial electric field is thus a flux surface average. However, as discussed in Sec. II, any variations of electrostatic potential Φ on a given flux surface are likely to be rapidly shorted out due to the very high mobility of electrons parallel to the magnetic field: the fact that measured electron density profiles in tokamaks never exhibit strong asymmetry about the magnetic axis indicates that the flux surface variation of $e\Phi$ must be of the order of the electron temperature or less.[14] Thus, we assume that the fast ion orbits are determined by a prescribed equilibrium magnetic field and the flux surface-averaged radial electric field. We set $\Phi=0$ throughout the plasma at $t=0$; Φ subsequently remains zero at the plasma boundary ($\Psi=\Psi_{\max}=\Psi_s$). The magnetic field is taken to be given by an analytical solution of the Grad-Shafranov equation obtained by Solov'ev:[26] the parameters of the solution are chosen to follow the convention adopted in the analysis presented in Sec. II, so that Ψ ranges from zero at the magnetic axis to $\Psi_{\max}$ at the edge.

A. MAST simulation

For the MAST simulation, the following parameters were used: major radius $R_0=0.86$ m, minor radius $a=0.53$ m (defined such that $2a$ is the total plasma width in the midplane), elongation $\kappa=1.7$, toroidal field $B_0=0.5$ T, and plasma current $I_p=586$ kA. A relatively low value was chosen for the current in order to maximize the radial excursions of the fast ions. More than 2×10^5 ions were injected over 5 ms, simulating a unidirectional beam of 40 keV deuterons ($A_f=2$, $Z_f=1$) injected in the direction counter to the plasma current at a constant rate of 3×10^{20} s^{-1}. The spatial birth profile was identical to that used in Ref. 14: all the ions were injected into trapped orbits, and drifted toward the edge of the plasma. The center of the source distribution was located in the midplane at a minor radial distance outboard of the magnetic axis approximately equal to $a/3$. The trapped orbit widths were such that all injected ions exited from the plasma, and could be lost due to charge exchange with neutral atoms: the average lifetime outside the plasma was taken to be 15 μs. With these parameters, more than 60% of the injected fast ions were lost during the 5 ms of the simulation. The flux surface-averaged fast ion current with zero radial electric field had a maximum value of 0.3 Am^{-2}. As discussed earlier, the electric field evolution was computed using the collisionless permittivity $\epsilon=\epsilon_0[1+c^2/c_A^2(\Psi)]$, as determined by the equilibrium magnetic field and a model bulk deuterium density profile $n(\Psi)=\mathrm{A}[1-(\Psi/\Psi_{max})^2]+\mathrm{B}$, where A and B are constants such that the density was equal

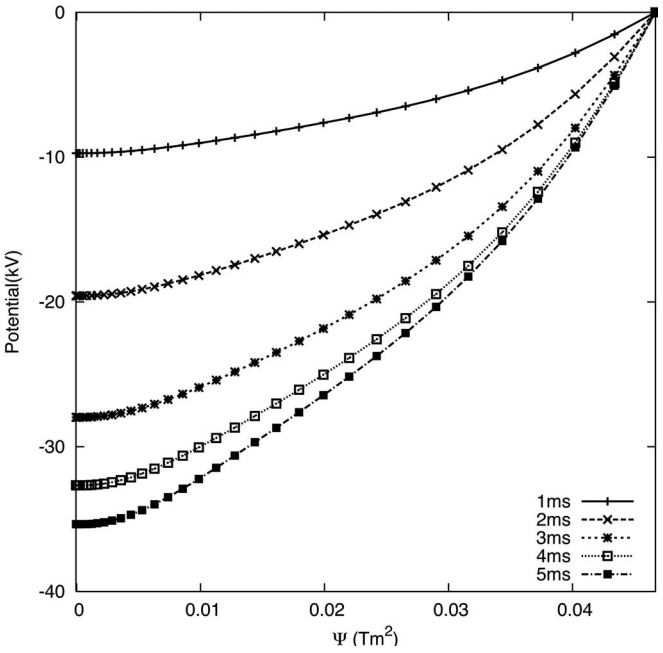

FIG. 1. TOPAS calculations of electrostatic potential Φ as a function of Ψ and time in a MAST-like plasma with countercurrent NBI. The magnetic axis is located at the point where $\Psi=0$.

to 3×10^{19} m^{-3} at the magnetic axis and 10% of this value at the plasma edge. The plasma permittivity typically decreases with minor radius. It is, however, equal to $3\times10^3\epsilon_0$ or more throughout the plasma, and so the return current almost completely cancels the fast ion current everywhere.

Nevertheless, as shown in Fig. 1, the imbalance between the two currents is sufficient to cause $|Z_f e\Phi|$ at the magnetic axis to rise to a value approaching the kinetic energy of the beam ions at birth on a time scale of a few milliseconds. The fast ions thus encounter a quasisteady radial electric field, and become increasingly confined by it. The drop in Φ implies a rise in the toroidal plasma rotation rate; in the ideal MHD limit represented by Eq. (47), the angular rotation rate is equal to $d\Phi/d\Psi$, i.e., the gradient of the curves in Fig. 1.

Figure 2 shows the cumulative number of ions injected (solid curve) and the cumulative number of ions lost from the plasma (dashed curve). The loss rate (the gradient of the dashed curve in Fig. 2) is initially almost equal to the injection rate, but starts decreasing significantly at $t\simeq2$ ms, when the central potential $\Phi(0)$ reaches -20 kV, and almost drops to zero at $t=5$ ms, when $\Phi(0)$ reaches -35 kV. At this point, the insulating scenario discussed in Ref. 14 has effectively been realized.

The central potential in high-performance countercurrent NBI MAST discharges has been estimated to be about -12 kV.[8] The key reason that this differs substantially from the saturated value of $\Phi(0)$ in Fig. 1 is that bulk ion dissipation was neglected in the simulation. The ion-ion collision time τ_{ii} in a high-performance MAST discharge is typically about 1 ms, and the neoclassical poloidal flow damping time $1/\nu_\theta\simeq(3r/2R)\tau_{ii}$ is somewhat shorter than this. On the 5 ms time scale of the MAST simulation, poloidal flow damping would in reality influence the temporal evolution of the ra-

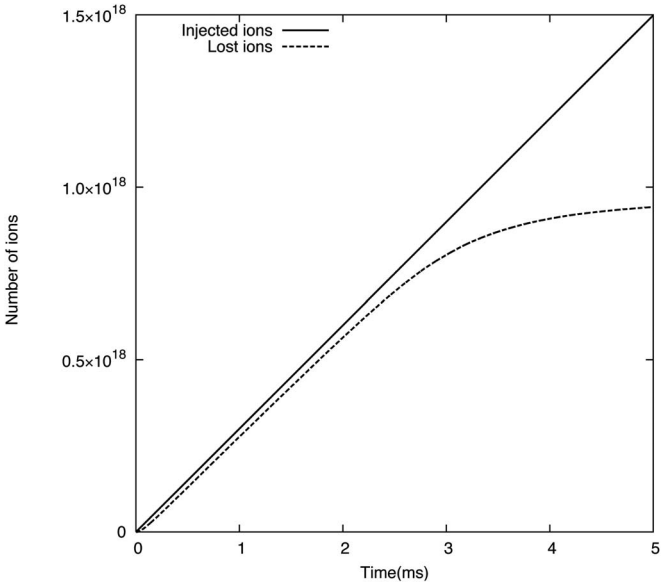

FIG. 2. Time evolution of the cumulative number of ions injected (solid curve) and the cumulative number of ions lost from the plasma (dashed curve) in the MAST-like simulation. The actual number of ions in the simulation (2×10^5) has been scaled up to a realistic value assuming an injection rate of 3×10^{20} s^{-1}.

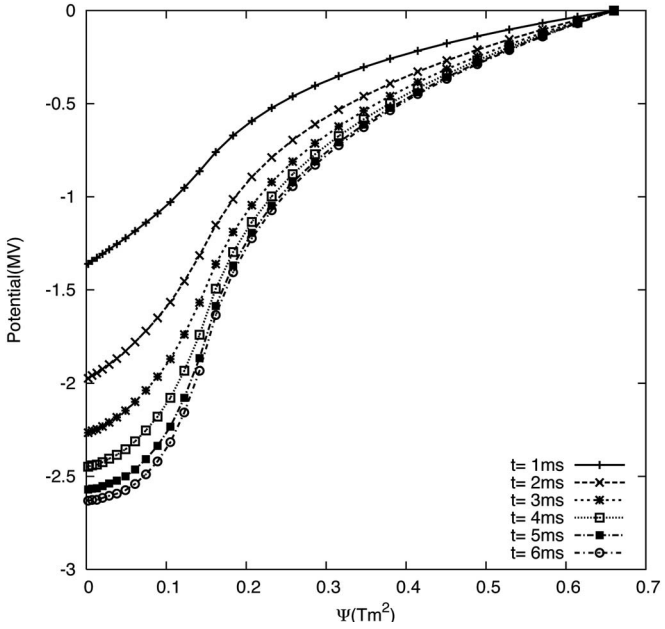

FIG. 3. TOPAS calculations of electrostatic potential Φ as a function of Ψ and time in a JET-like plasma with fusion α-particles. The magnetic axis is located at the point where $\Psi=0$. The α-particles are born within the region corresponding to $\Psi\leq0.16$ Tm^2.

dial electric field and cause it to saturate at a value comparable to that given by Eq. (36). Figure 1 shows how the electrostatic potential would evolve during countercurrent NBI in MAST if, *ceteris paribus*, the collisionality were to be significantly reduced. In future MAST operations, with increased NBI power and higher temperatures, it is possible that the limit $E\simeq E^{\mathrm{crit}}$ could be approached.

B. JET simulation

In the case of the JET simulation, the following parameters were used: $R_0=3$ m, $a=1$ m, $\kappa=1.7$, $B_0=2.3$ T, and $I_p=2.51$ MA. These parameters correspond approximately to those of a series of JET deuterium-tritium discharges in which ion cyclotron emission was observed.[27] This emission is known to be produced by fusion α-particles traversing the outer midplane edge of the plasma: centrally born α-particles were relatively poorly confined in these discharges because the plasma current was relatively low. The fusion power (<1 MW) was also relatively low compared to other discharges in the 1997 JET deuterium-tritium campaign. In JET, the time evolution would be prohibitively slow if the collisionless plasma permittivity were to be used, and the vacuum value was therefore used instead. To further expedite the rise of the radial electric field, an artificially high fusion power was assumed. Fusion α-particles were launched isotropically with kinetic energy 3.5 MeV at a constant rate in the central region of the plasma, corresponding to normalized minor radii $x\equiv(\Psi/\Psi_{\mathrm{max}})^{1/2}\leq0.5$. Within this core region, the α-particle birth probability was taken to be uniform. At the start of the simulation, the number of α-particles in the system was set equal to zero. Two electrons were introduced on a flux surface every time an α-particle was born on that surface, ensuring that the net aggregate charge launched into the system was zero. Poloidal flux was taken to be a constant of the motion for these electrons, and so space charge arose solely as a result of the orbital excursions of α-particles from flux surfaces. In the collisionless limit, the velocity distribution of fusion α-particles has been shown to be anisotropic close to the magnetic axis, even when the α-particle source is itself isotropic, due to trapped orbit effects.[28] Since full orbits were computed in the simulation, this effect was taken into account.

In total, 16000 fusion α-particles were launched into the plasma over a period of 6 ms. Figure 3 shows Φ as a function of Ψ and t for this scenario. At the start of the simulation, α-particles immediately migrate outside the central birth region and produce a local space charge that drives up the radial electric field. Some of the α-particles cross the plasma boundary at $\Psi=\Psi_{\mathrm{max}}$, and are deemed to be lost immediately from the system. At any given location in the plasma, it is apparent that Φ is a monotonic decreasing function of time, and therefore α-particle energies must decrease [cf. Eq. (16)]. The rate of increase of $|\Phi|$ and hence E slows down and approaches asymptotically a true steady state outside the fast particle birth region ($\Psi\geq0.16$ Tm^2). The potential at the edge of the α-particle production region tends to the value -1.75 MV, which is sufficient to confine electrostatically a 3.5 MeV α-particle born on that flux surface. For particles born closer to the magnetic axis, there is an even larger potential difference between the birth location and the plasma edge, and therefore all α-particles subsequently born in the plasma are confined. Inside the birth region Φ continues to evolve as more α-particles are born and, in some cases, migrate outside this region. However, there is a complete cessation of α-particle losses, as shown in Fig. 4.

Examining the trajectories of α-particles that are lost during this simulation, we find that some of them are born into confined passing orbits rather than trapped orbits. As the

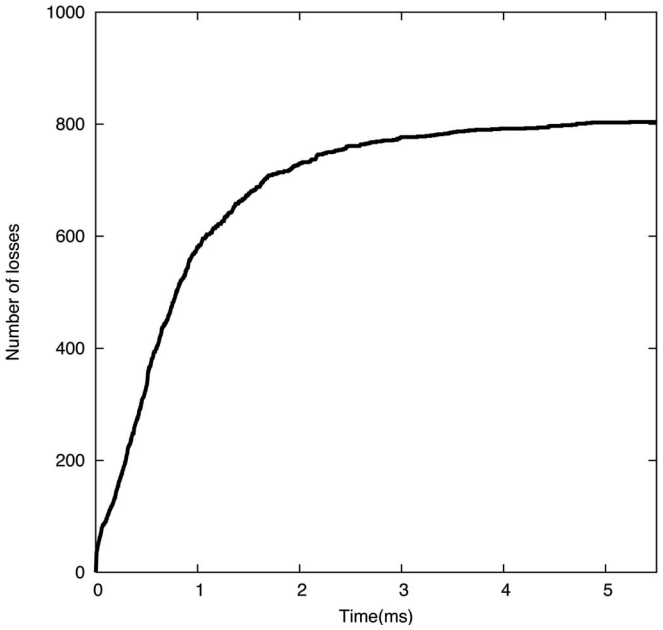

FIG. 4. Cumulative losses vs time of fusion α-particles in a JET-like plasma, simulated using TOPAS.

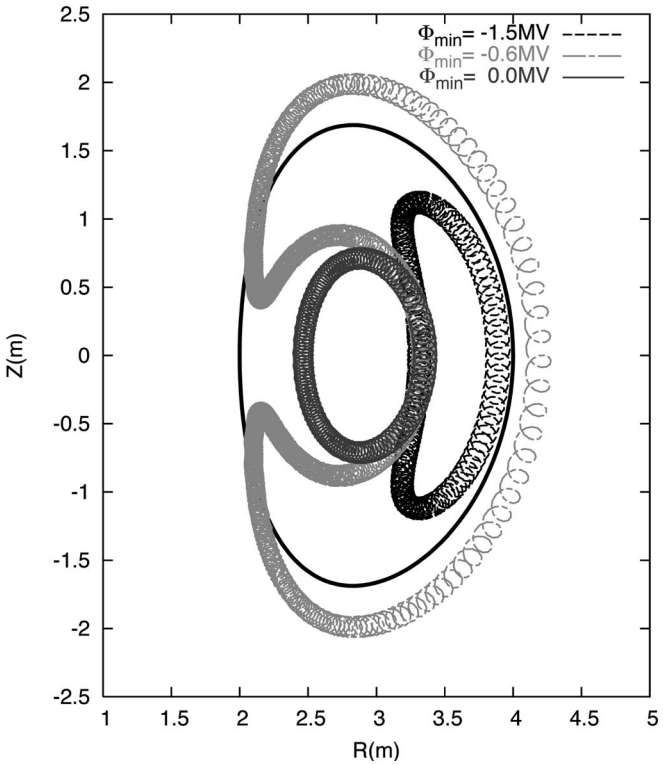

FIG. 5. Orbit of fusion α-particle born with $v_\zeta<0$ (the countercurrent direction) in a JET-like plasma, computed using TOPAS for different radial electric fields. The electrostatic potential was prescribed as a linear function of Ψ, with minimum value $\Phi_{\min}$ at the magnetic axis. The particle is passing for zero electric field (dark gray curve), but becomes trapped and crosses the plasma boundary (full black curve) when the potential is lowered (light gray curve). When the potential is lowered still further, the particle remains in a trapped orbit but is once again confined (dashed black curve).

radial electric field increases, the particles are lost either because their orbits became trapped, as in Fig. 5, or, in some cases, because their passing orbits intersect the inboard plasma edge. Thus, delayed losses occur in addition to the prompt losses arising from trapped particles crossing the last closed flux surface in their first bounce orbit, and the total loss rate is higher than might have been expected. A further increase in the radial electric field causes the trapped orbits to shrink, so that the full orbits again lie inside the plasma boundary and the particle is confined.

We emphasize that this is not a realistic simulation of a JET plasma since, in addition to neglecting the bulk ion polarization current, we have used an artificially high fusion power. In reality, the radial currents due to α-particles in JET deuterium-tritium discharges were much too low for E to approach E^{crit} [cf. Eq. (32)]. However, Figs. 3–5 serve to illustrate the fact that fusion α-particle losses, in the absence of dissipative effects, can in principle drive up radial electric fields that confine electrostatically α-particles remaining in the plasma. The localized steepening of $\Phi(\Psi)$ close to the edge of the α-particle birth region in Fig. 3 also illustrates the point that radial fast particle currents can produce strongly sheared radial electric fields, which play a key role in the formation of transport barriers. Minority ions heated to MeV energies using ICRF waves could in principle be used to create and control such barriers at specific locations in the plasma via the collisionless electrodynamic process discussed in this paper.

C. ITER simulations

Finally, a set of simulations corresponding to ITER-like plasmas were performed, with $R_0=6$ m, $a=2$ m, $\kappa=1.8$, and $B_0=5.3$ T. In one of these simulations, aimed at studying the mechanisms underlying the existence of the current, the α-particle source was localized to a single flux surface. Three other simulations were performed with the aim of estimating the current density for the case of a realistic α-particle birth profile and a range of values of the plasma current ($I_p=10-20$ MA).

Unlike neutral beam-injected fast ions, fusion α-particles in a thermonuclear deuterium-tritium plasma are distributed isotropically in velocity space and can thus drift radially inward or outward (with equal probability) from their birth position. Figure 6 shows the final flux surface-averaged electric polarization per α-particle resulting from the injection at $t=0$ of 100000 α-particles at $\Psi/\Psi_{\max}=0.5$. In this simulation, the plasma current was taken to be 15 MA. Polarization results from the fact that the α-particles migrate from the flux surface on which they are born. From the moment of injection, there are radial currents directed both inward and outward from the birth flux surface source; these currents eventually vanish, but there remains a net flux surface-averaged electric polarization $\langle P\rangle$, determined by the time-integrated current,

$$\langle P\rangle \equiv \frac{1}{A(\Psi)}\oint_\Psi \mathbf{P}(t)\cdot\mathbf{n}dA = -\frac{1}{A(\Psi)}\int_V \rho(t)dV$$
$$= \frac{1}{A(\Psi)}\int_0^t \left(\oint \mathbf{j}_f(t')\cdot\mathbf{n}dA\right)dt', \tag{48}$$

where $\mathbf{P}$ is the local electric polarization, ρ is charge density,

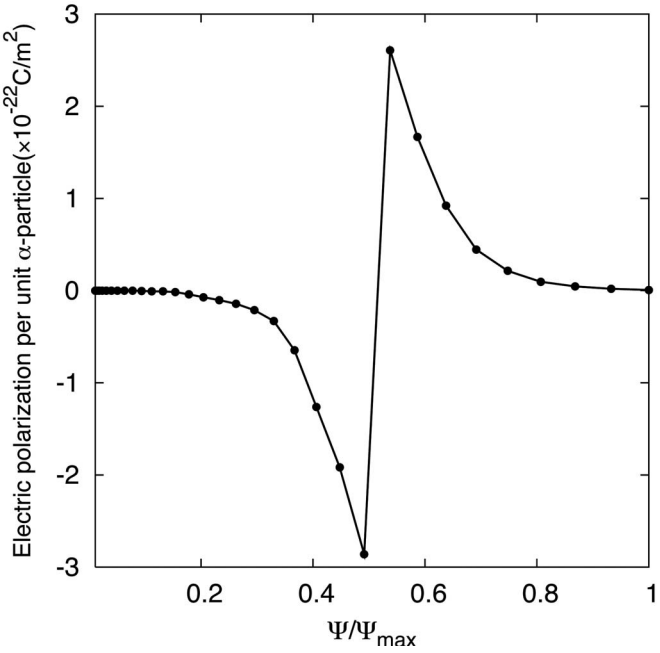

FIG. 6. Steady-state flux surface-averaged electric polarization per α-particle computed from a test-particle simulation of fusion α-particle orbits in an ITER-like plasma. At $t=0$, 100000 α-particles were injected at $\Psi/\Psi_{max}=0.5$; no further α-particles were injected after $t=0$. The magnetic axis lies at $\Psi=0$.

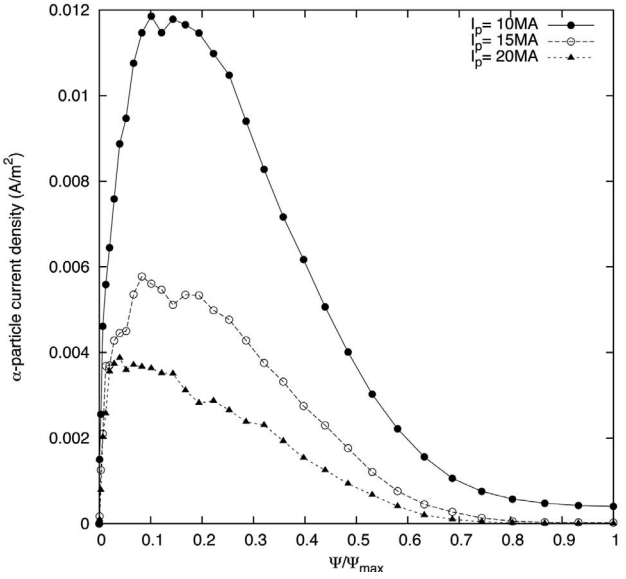

FIG. 7. Time-averaged radial current due to fusion α-particles for three values of the plasma current in ITER-like plasmas. The magnetic axis lies at $\Psi=0$.

$\mathbf{j}_f$ is the α-particle current, V is the volume enclosed by flux surface Ψ, and we have used the equation of charge conservation. Figure 6 shows $\langle P \rangle$ in the limit $t \to \infty$. The shape of the curve in this figure can be understood in the following terms. Inward-drifting α-particles produce an aggregate positive charge (and hence a negative polarization) inside the birth flux surface, since the two electrons introduced into the plasma with each α-particle remain on that flux surface. The volume-integrated charge has a discontinuity at $\Psi=0.5\Psi_{max}$ and is negative immediately outside this surface, since some of the α-particles drift outside the enclosed volume. The total charge and polarization tend to zero toward the edge, since no α-particles are lost from the plasma. This indicates that a localized source of fast ions with an isotropic velocity distribution can produce shear flows, the rotation being driven by a torque that changes sign at the birth flux surface.

A full α-particle birth distribution can be regarded as an integral over localized distributions, each producing an electric polarization profile of the type shown in Fig. 6. If the strength of the localized source decreases with Ψ, it is clear that there will be a net positive current and polarization. To quantify this net current, three test-particle simulations were performed with 10^5 fusion α-particles injected over 250 μs into ITER-like equilibria with plasma currents of 10, 15, and 20 MA. The actual plasma current in projected ITER scenarios ranges from around 10 MA for steady-state operation to 15 MA for inductive operation;[29] the 20 MA simulation was performed in order to bring out more clearly the scaling of fast ion current with plasma current.

It is important to note that a key feature of the steady-state ("advanced") scenario in ITER is that q is not a monotonic increasing function of Ψ, i.e., there are regions of reversed magnetic shear in the plasma. This shear reversal cannot be represented, however, in our simple equilibrium model. Fusion α-particle orbits and the corresponding radial current will of course depend on the details of the equilibrium, not merely on the plasma current, and therefore the values we obtain for the radial current in the 10 MA case should be treated with some caution. Since these were test-particle simulations, the electric field resulting from α-particle orbital excursions was not taken into account, and moreover no α-particles were lost except for the lowest value of the current. To compute the α-particle birth profile, the fuel ion temperature was assumed to decrease linearly with Ψ from 23 keV at the magnetic axis to zero at the plasma edge; the fuel ion density was assumed to be constant. The birth probability was evaluated using the analytical approximation to the fusion reaction rate obtained by Brysk.[30]

The time-averaged α-particle current density is plotted versus Ψ for each of the three scenarios in Fig. 7. Because some of the particles are lost when $I_p=10$ MA, there is a finite current density at the plasma boundary in this case. In the other two cases, the α-particles are all confined. In practice, losses of α-particles from ITER, and thus to some extent the radial α-particle current, are likely to be determined largely by toroidal field ripple effects, which are not modeled in these simulations since the plasma equilibria are axisymmetric. The loss rate due to such effects is predicted to be rather low in the inductive mode of operation, around 2% or less,[31,32] but it could be as high as 20% in the steady-state mode.[31] Even without this additional loss channel, it is evident from Fig. 7 that the fast particle current is significantly higher in the steady-state scenario ($I_p=10$ MA) than it is in the inductive case ($I_p=15$ MA). The peak fast particle current scales approximately as $1/I_p^2$. This scaling can be understood qualitatively as follows. The electric dipole moment produced by each trapped α-particle is $Z_f e \Delta$, where Δ

$\sim (r/R)^{1/2}\rho_{f\theta}$ is the particle orbit width, r being minor radial distance and $\rho_{f\theta}$ poloidal Larmor radius. Since the fraction of particles in trapped orbits is approximately $(r/R)^{1/2}$, it follows that the net polarization on a particular flux surface resulting from α-particle production is

$$\delta P \sim Z_f e\left(\frac{r}{R}\right)^{1/2}[n_f(r+\Delta)-n_f(r-\Delta)]\Delta$$
$$\sim Z_f e\rho_{f\theta}^2\left(\frac{r}{R}\right)^{3/2}\frac{\partial n_f}{\partial r}, \tag{49}$$

where n_f is the α-particle number density. If the α-particles are born in a time δt, the corresponding current density is

$$j \sim \frac{\delta P}{\delta t} \sim Z_f e\rho_{f\theta}^2\left(\frac{r}{R}\right)^{3/2}\frac{\partial \dot{n}_f}{\partial r}, \tag{50}$$

where $\dot{n}_f$ is the α-particle birth rate per unit volume. Passing α-particles also contribute to this current, and are more numerous than trapped particles by a factor of order $(R/r)^{1/2}$. However, since Δ for these particles is smaller than that of trapped particles by a similar factor, and $j \propto \Delta^2$, the passing particle contribution to the radial current is around $(R/r)^{1/2}$ times smaller than the trapped particle contribution. However, both contributions scale as $1/I_p^2$.

The currents in Fig. 7 are relatively small compared with those found in the MAST simulation (≤ 0.3 Am^{-2}), and the corresponding radial electric fields are much smaller than the critical values required for electrostatic confinement. From Eq. (34), we infer that the steady-state toroidal velocity is then given by

$$v_\zeta \simeq -\frac{j_f^*(0)B_\theta}{\rho_m \nu_\zeta}. \tag{51}$$

Evaluating the right-hand side of this expression with $j_f^*(0)$ given by the peak values of the α-particle current in Fig. 7, using appropriate values of B_θ and ρ_m, and identifying $1/\nu_\zeta$ with the projected energy confinement times in the two scenarios,[29] we obtain $v_\zeta \simeq -25$ km s^{-1} (inductive operation) and $v_\zeta \simeq -50$ km s^{-1} (steady-state operation). Although relatively modest compared to the velocities routinely observed in smaller devices, these figures suggest that plasma rotation due to fusion α-particle currents in ITER may be sufficient to affect significantly the stability of MHD modes such as NTMs[4] and RWMs.[5] It should also be noted that ITER plasmas will contain substantial fast particle populations in addition to fusion α-particles, particularly in the steady-state scenario for which the projected α-particle power is approximately equal to the auxiliary heating and current drive power.[29] Thus, the total fast particle radial current could be significantly higher than the α-particle current plotted in Fig. 7. Moreover, if turbulence were to drive a significant trapped α-particle diffusion current, as suggested earlier, larger electric fields and rotation velocities would be possible.

Transport calculations indicate that the collisional torque due to neutral beams in the ITER steady-state scenario would produce a (cocurrent) toroidal rotation velocity in the plasma core of around 140 km s^{-1},[33] which is close to the value required for RWM stabilization.[5] However, this estimate of v_ζ must be offset by the rotation rate associated with the fast ion current $j_f^*(0)$, since this is always counter to the plasma current whenever $j_f^*(0) > 0$. Our estimates of the α-particle current alone suggest that the offset should be taken into account in assessing MHD stability in ITER. In this context, it is worth remarking that countercurrent NBI in ITER would produce a countercurrent torque; this would be augmented rather than offset by the collisionless α-particle torque, and could therefore be advantageous for MHD stability and confinement.

Rosenbluth and Hinton[34] used the drift kinetic equation to estimate analytically the toroidal rotation velocity likely to be driven by α-particles in a tokamak reactor. For the case of a constant fusion reaction rate, they concluded that a significant net (intrinsic) radial α-particle current would only be present for a slowing-down time τ_{slow} after the start of α-particle production [cf. Eq. (51) in Ref. 34]. Since it would take a time of order $1/\nu_\zeta \gg \tau_{\text{slow}}$ for the plasma to be accelerated by a steady fast ion current to the toroidal velocity given by Eq. (51), Rosenbluth and Hinton concluded that the maximum α-particle-driven rotation rate would be smaller than this value, by a factor of order $1/\tau_{\text{slow}}\nu_\zeta$, and that such low rotation rates would have a negligible impact on MHD stability. However, we believe that the calculation presented in Ref. 34 is incomplete because it does not take account of the fact that every α-particle born in the plasma contributes to the intrinsic fast particle current, irrespective of the temporal evolution of the birth rate or the number of slowing-down times that have elapsed since the start of α-particle production. Rosenbluth and Hinton employ an ordering in which the leading order α-particle distribution function is determined entirely by the birth rate and slowing-down, with drift orbit excursions playing no role [see Eq. (25) in Ref. 34]. To compute the intrinsic α-particle current and hence the return current torque, it is appropriate to solve the full Vlasov equation, as we have done in this paper.

IV. CONCLUSIONS AND DISCUSSION

We have investigated collective fast ion effects on toroidal and poloidal flows in tokamaks using a combination of analytical and numerical techniques. Following on from the analysis presented in Ref. 14, we have developed a simple unified model of electrodynamic momentum transfer from collisionless fast ions to bulk plasma, taking into account bulk ion polarization currents and dissipation. For the case of large aspect ratio toroidal geometry, we have solved analytically the initial value problem of bulk plasma spin-up driven by fast ion radial currents. We have illustrated our analysis using idealized simulations of fast ion orbits and radial electric fields in MAST, JET, and ITER. In the MAST and JET simulations, the flux surface-averaged form of Poisson's equation was solved simultaneously with the fast ion orbit equations, while test-particle simulations were performed for ITER-like plasmas. In the case of MAST, prompt losses of beam ions injected counter to the plasma current were found to drive up a radial electric field that saturated at a level such that beam ions subsequently injected were confined electrostatically. Bulk ion momentum balance in the presence of

such a field implies a countercurrent toroidal plasma velocity of the order of 1500 km s^{-1}. Although the actual rotation rates in counterinjected MAST plasmas are lower than this, the scenario explored in the simulation would be realized in MAST if the bulk ion collision frequency were to be reduced by a factor of around 5 or more, for example by increasing the neutral beam heating power. The JET simulation, although unrealistic (the assumed fusion power was artificially high and the bulk plasma polarization current was neglected), shows that a similar process would occur in a burning plasma with a sufficiently high fusion α-particle production rate, and also illustrate the fact that fast ions with steep birth profiles can produce highly sheared electric fields, which are known to be associated with the suppression of turbulent transport. In one of the ITER simulations, drift orbit excursions of fusion α-particles launched simultaneously from a single flux surface were shown to produce a permanent electric polarization in the plasma. Continuous fast particle production, with a spatial gradient in the birth probability, produces a radial current that is associated with this polarization effect and is thus essentially collisionless. Other simulations were performed with the aim of estimating the radial currents due to fusion α-particles in the inductive and steady-state modes of operation in ITER. These estimates imply that the stability of NTMs and RWMs is likely to be significantly affected in ITER by flows associated with radial fast ion currents; if the toroidal rotation were driven primarily by the collisional torque of co-injected neutral beams, the fast ion currents would have a destabilizing effect.

Some interesting general perspectives are suggested by the model. It is well known that mechanical angular momentum is not conserved in the presence of electromagnetic fields since the Lorentz force on a moving charge is not a central force. Indeed, the operation of dynamos and electric motors relies entirely on this phenomenon. A conductor moving in a quasistatic magnetic field induces an electric field transverse to both the motion and the magnetic field, an effect that is fundamental to MHD: this is the essential principle of the dynamo. Conversely, a changing electric field in a static magnetic environment will tend to drive motions in a conductor—an effect exploited in electric motors. Our model indicates that radial electric fields can be created by adding fast ions to a quasineutral plasma, which responds both reactively and resistively. In typical tokamak conditions, it should be possible to affect the toroidal rotation of the plasma by this means, as demonstrated experimentally using neutral beams in DIIID.[9] In that experiment, however, the incoming fast ions also carried momentum, which could only be delivered to the plasma via collisions. When the fast ions are isotropically born fusion α-particles or ICRF-heated minority ions with energies in the MeV range, there is no net injection of momentum. The possibility of spinning up a plasma in these circumstances can be compared with the bootstrap method of current drive, which requires only a pressure gradient, two species of electrons (trapped and passing), and low collisionality. Thus, fast ion production (provided either externally or via fusion reactions) can, in effect, turn a tokamak plasma into an electric motor. We suggest that practical calculations should be undertaken using the principles elucidated in this paper with the aim of modeling electric field generation and flows in both ITER and spherical tokamak reactors.[35]

ACKNOWLEDGMENTS

We thank an anonymous referee for stimulating comments and suggestions that have led to improvements in the paper. This work was supported by the Engineering and Physical Sciences Research Council and by the European Communities under the Contract of Association between EURATOM and UKAEA. The views and opinions expressed herein do not necessarily reflect those of the European Commission.

APPENDIX: ENERGY AND ANGULAR MOMENTUM CONSERVATION IN TOKAMAK PLASMAS WITH FAST PARTICLES

For definiteness, we consider a tokamak plasma in which the only fast particles are produced by NBI. However, the analysis is applicable to any fast particle population that is collisionless and perfectly confined in the plasma.

Suppose N_f neutral beam atoms are injected instantaneously (in a "blip") into a tokamak magnetic field of the form $\mathbf{B}=\nabla\zeta\times\nabla\Psi+RB_\zeta\nabla\zeta$, where B_ζ is toroidal field. When the atoms are ionized, the ions produce an electric field due to orbit excursions from the flux surface on which they are born, but we assume that they do not modify the magnetic field. The beam electrons, by virtue of their small mass, do not undergo significant orbit excursions and have negligible energy. Neglecting for the time being the bulk plasma and assuming that all the ions are confined in the plasma, one can easily deduce the following energy conservation relation:

$$\varepsilon_f^{\mathrm{in}}=\varepsilon_f+\varepsilon_{\mathrm{field}}\equiv\int\frac{1}{2}A_f m_p\mathbf{v}^2F_f d\mathbf{v}d\mathbf{x}+\frac{\epsilon_0}{2}\int\mathbf{E}\cdot\mathbf{E}d\mathbf{x}, \tag{A1}$$

where $\varepsilon_f^{\mathrm{in}}$, ε_f, and $\varepsilon_{\mathrm{field}}$ are, respectively, the total energy of the beam atoms, the kinetic energy of the beam ions, and the electrostatic field energy, and the integrals are over velocity space and the plasma volume. To establish this result, we multiply the fast ion Vlasov equation [Eq. (15)] by $A_f m_p\mathbf{v}^2/2$ and evaluate the appropriate integrals, obtaining

$$\frac{d}{dt}\left(\int\frac{1}{2}A_f m_p\mathbf{v}^2F_f d\mathbf{v}d\mathbf{x}\right)\equiv\frac{d\varepsilon_f}{dt}=\int\mathbf{j}_f\cdot\mathbf{E}d\mathbf{x}. \tag{A2}$$

In deriving this result, we have invoked the assumption that no fast ions are lost from the plasma, so that $F_f=0$ at the plasma boundary, and we have also neglected the source term in the Vlasov equation since $S_f=0$ after the initial instantaneous injection of the beam. Taking the scalar product of Ampère's law with $\mathbf{E}$ and integrating over the plasma volume, using the fact that $\mathbf{j}_f$ is the only part of the conduction current that is not balanced by $\nabla\times\mathbf{B}$ and assuming zero Poynting flux on the plasma boundary (this is equivalent to assuming that the fast ions are confined), we find moreover that

$$\frac{d}{dt}\left(\frac{\epsilon_0}{2}\int E^2 d\mathbf{x}\right) \equiv \frac{d\varepsilon_{\text{field}}}{dt} = -\int \mathbf{j}_f \cdot \mathbf{E} d\mathbf{x}. \tag{A3}$$

Adding Eqs. (A2) and (A3), we obtain

$$\frac{d}{dt}(\varepsilon_f + \varepsilon_{\text{field}}) = 0,$$

and hence, since the electrostatic field energy is initially zero,

$$\varepsilon_f(t) + \varepsilon_{\text{field}}(t) = \varepsilon_f^{\text{in}}.$$

With suitable modifications to the definitions of ε_f and $\varepsilon_{\text{field}}$, this result remains valid when electrons and time-dependent magnetic fields are taken into account, provided that radiation losses are negligible.

An angular momentum conservation law for this system can be established in a similar fashion. Denoting by L_f^ζ and L_{field}^ζ the toroidal angular momentum of the fast ions and the field, respectively, we have

$$L_f^\zeta = \int A_f m_p R v_\zeta F_f d\mathbf{v} d\mathbf{x}$$

and

$$L_{\text{field}}^\zeta = \int R\epsilon_0 (\mathbf{E}\times\mathbf{B})\cdot(R\nabla\zeta) d\mathbf{x}.$$

The expression for L_{field}^ζ follows from the result that the momentum density associated with an electromagnetic field is equal to energy flux density $S \equiv \epsilon_0 c^2 \mathbf{E}\times\mathbf{B}$ divided by c^2.[36] Multiplying the Vlasov equation by $A_f m_p R v_\zeta$, integrating over phase space, and using $\mathbf{B} = \nabla\zeta\times\nabla\Psi + RB_\zeta\nabla\zeta$, we find that

$$\frac{dL_f^\zeta}{dt} = \int R^2 \nabla\zeta\cdot(\mathbf{j}_f\times\mathbf{B}) d\mathbf{x} = \int R j_f^\Psi B_\theta d\mathbf{x}. \tag{A4}$$

The right-hand side of this equation represents the toroidal torque on the fast ion population resulting from the motion of those ions across flux surfaces. The rate of change of field angular momentum is given by

$$\begin{aligned}\frac{dL_{\text{field}}^\zeta}{dt} &= \frac{d}{dt}\left(\int R^2\epsilon_0 \mathbf{E}\times\mathbf{B}\cdot\nabla\zeta d\mathbf{x}\right)\\ &= \int R^2\epsilon_0 \frac{\partial\mathbf{E}}{\partial t}\times\mathbf{B}\cdot\nabla\zeta d\mathbf{x}\\ &= -\int R j_f^\Psi B_\theta d\mathbf{x},\end{aligned} \tag{A5}$$

where we have again used Ampère's law. It follows from Eqs. (A4) and (A5) that

$$\frac{d}{dt}(L_f^\zeta + L_{\text{field}}^\zeta) = 0, \tag{A6}$$

i.e., total angular momentum is conserved; there is a transfer of angular momentum from beam atoms to the field when the former are ionized.[13] Thus, the neutral beam does not deliver all of its angular momentum to confined charged particles. In particular, a large fraction of the angular momentum residing in beam ions at the moment of birth can be transferred to the field.

Similar results can be established for the case in which fast ions and associated electrons are injected into a quasineutral plasma with a single bulk ion species and massless electrons. We assume as before that the injection does not modify the magnetic field structure, that all injected and bulk plasma particles are confined, and that collisions can be neglected. Energy conservation of the system comprising fast ions, bulk ions, and field can be demonstrated by combining Eq. (A2) with a similar result for the bulk ions,

$$\frac{d}{dt}\left(\int \frac{1}{2} A_i m_p \mathbf{v}^2 F_i d\mathbf{v} d\mathbf{x}\right) = \int \mathbf{j}_i\cdot\mathbf{E} d\mathbf{x}, \tag{A7}$$

and Ampère's law in the form

$$\epsilon_0 c^2 \nabla\times\mathbf{B} = \mathbf{j}_f + \mathbf{j}_i + \epsilon_0\frac{\partial\mathbf{E}}{\partial t},$$

to obtain

$$\frac{d}{dt}\left(\frac{\epsilon_0}{2}\int \mathbf{E}\cdot\mathbf{E} d\mathbf{x}\right) = -\int (\mathbf{j}_f + \mathbf{j}_i)\cdot\mathbf{E} d\mathbf{x}. \tag{A8}$$

Summing Eqs. (A2), (A7), and (A8), we obtain the required result. In this scenario, there is a plasma displacement current with a dielectric constant that is much larger than the vacuum value, and the field does work on the bulk ions. It is straightforward to show that the ratio of bulk ion energy to electric field energy is essentially equal to c^2/c_A^2. Thus, almost all of the energy lost from the fast ions is channeled into the bulk ions, with only a small fraction remaining in the field. Note that this exchange of energy is mediated entirely by the field as it builds up; there is no collisional transfer of momentum. However, since the polarization is due mainly to trapped particles, only a fraction of the input energy is transferred to the bulk plasma.

We consider finally angular momentum conservation in the collisionless limit with bulk ions taken into account. These ions have toroidal angular momentum

$$L_i^\zeta = \int A_i m_p R v_\zeta F_i d\mathbf{v} d\mathbf{x},$$

while L_f^ζ and L_{field}^ζ are defined as before. Multiplying the bulk ion Vlasov equation by $A_i m_p R v_\zeta$ and integrating over phase space, we obtain a result analogous to Eq. (A4),

$$\frac{dL_i^\zeta}{dt} = \int R^2 \nabla\zeta\cdot(\mathbf{j}_i\times\mathbf{B}) d\mathbf{x} = \int R j_i^\Psi B_\theta d\mathbf{x}. \tag{A9}$$

It is straightforward to show that the rate of change of field angular momentum is now given by

$$\frac{dL_{\text{field}}^\zeta}{dt} = -\int R(j_f^\Psi + j_i^\Psi) B_\theta d\mathbf{x} \tag{A10}$$

using Maxwell's equations. It follows from Eqs. (A4), (A9), and (A10) that

$$\frac{d}{dt}(L_f^\zeta + L_i^\zeta + L_{\text{field}}^\zeta) = 0,$$

i.e., total angular momentum is conserved. As in the case of energy, only a fraction of the input angular momentum is lost from the beam in the absence of collisions, and the ratio of angular momentum transferred to the bulk plasma to that transferred to the field is essentially equal to c^2/c_A^2. When bulk ion collisions are taken into account, energy and angular momentum are transported out of the system; the conservation laws derived above can be generalized to include the effects of energy and angular momentum fluxes at the plasma boundary.

[1] I. T. Chapman, T. C. Hender, S. Saarelma, S. E. Sharapov, R. J. Akers, N. J. Conway, and the MAST Team, Nucl. Fusion **46**, 1009 (2006).
[2] S. D. Scott, P. H. Diamond, R. J. Fonck, R. J. Goldston, R. B. Howell, K. P. Jaehnig, G. Schilling, E. J. Synakowski, M. C. Zarnstorff, C. E. Bush, E. Fredrickson, K. W. Hill, A. C. Janos, D. K. Mansfield, D. K. Owens, H. Park, G. Pautasso, A. T. Ramsey, J. Schivell, G. D. Tait, W. M. Tang, and G. Taylor, Phys. Rev. Lett. **64**, 531 (1990).
[3] R. Aymar, V. A. Chuyanov, M. Huguet, Y. Shimomura, ITER Joint Central Team, and ITER Home Teams, Nucl. Fusion **41**, 1301 (2001).
[4] A. M. Popov, *Proceedings of the 33rd EPS Conference on Plasma Physics*, edited by F. De Marco and G. Vlad (European Physical Society, Rome, 2006), Vol. 30I, p. 1.106.
[5] Y. Liu, M. S. Chu, A. M. Garofalo, R. J. La Haye, Y. Gribov, M. Gryaznevich, T. C. Hender, D. F. Howell, P. de Vries, M. Okabayashi, S. D. Pinches, H. Reimerdes, and EFDA-JET Contributors, Phys. Plasmas **13**, 056120 (2006).
[6] N. C. Hawkes and N. J. Peacock, Nucl. Fusion **25**, 971 (1985).
[7] F. L. Hinton and M. N. Rosenbluth, Phys. Lett. A **259**, 267 (1999).
[8] R. J. Akers, P. Helander, A. Field, C. Brickley, D. Muir, N. J. Conway, M. Wisse, A. Kirk, A. Patel, A. Thyagaraja, C. M. Roach, and the MAST and NBI Teams, *Proceedings of the 20th IAEA Fusion Energy Conference* (International Atomic Energy Agency, Vienna, 2005), EX/4-4.
[9] J. S. deGrassie, R. J. Groebner, and K. H. Burrell, Phys. Plasmas **13**, 112507 (2006).
[10] L.-G. Eriksson, E. Righi, and K.-D. Zastrow, Plasma Phys. Controlled Fusion **39**, 27 (1997).
[11] J. E. Rice, M. Greenwald, I. H. Hutchinson, E. S. Marmar, Y. Takase, S. M. Wolfe, and F. Bombarda, Nucl. Fusion **38**, 75 (1998).
[12] F. W. Perkins, R. B. White, P. T. Bonoli, and V. S. Chan, Phys. Plasmas **8**, 2181 (2001).
[13] P. Helander, R. J. Akers, and L.-G. Eriksson, Phys. Plasmas **12**, 112503 (2005).
[14] K. G. McClements and A. Thyagaraja, Phys. Plasmas **13**, 042503 (2006).
[15] T. H. Stix, Nucl. Fusion **15**, 737 (1975).
[16] F. L. Hinton and Y.-B. Kim, Phys. Fluids B **5**, 3012 (1993).
[17] R. C. Morris, M. G. Haines, and R. J. Hastie, Phys. Plasmas **3**, 4513 (1996).
[18] F. L. Hinton and M. N. Rosenbluth, Plasma Phys. Controlled Fusion **41**, A653 (1999).
[19] M. N. Rosenbluth, P. H. Rutherford, J. B. Taylor, E. A. Frieman, and L. M. Kovrizhnikh, *Plasma Physics and Controlled Nuclear Fusion Research 1971* (International Atomic Energy Agency, Vienna, 1971), Vol. 1, p. 495.
[20] N. Winsor, J. L. Johnson, and J. M. Dawson, Phys. Fluids **11**, 2448 (1968).
[21] S. V. Novakovskii, C. S. Liu, R. Z. Sagdeev, and M. N. Rosenbluth, Phys. Plasmas **4**, 4272 (1997).
[22] F. L. Hinton and R. D. Hazeltine, Rev. Mod. Phys. **48**, 239 (1976).
[23] F. L. Hinton and J. A. Robertson, Phys. Fluids **27**, 1243 (1984).
[24] A. B. Rechester and M. N. Rosenbluth, Phys. Rev. Lett. **40**, 38 (1978).
[25] F. Schwander, Ph.D. thesis, Imperial College London (2007).
[26] L. S. Solov'ev, Sov. Phys. JETP **26**, 400 (1968).
[27] K. G. McClements, C. Hunt, R. O. Dendy, and G. A. Cottrell, Phys. Rev. Lett. **82**, 2099 (1999).
[28] V. Ya. Goloborod'ko, Y. I. Kolesnichenko, and V. A. Yavorkskij, Nucl. Fusion **23**, 399 (1983).
[29] *ITER Technical Basis* (International Atomic Energy Agency, Vienna, 2001).
[30] H. Brysk, Plasma Phys. **15**, 611 (1973).
[31] S. V. Konovalov, E. Lamzin, K. Tobita, and Yu. Gribov, in *Proceedings of the 28th EPS Conference on Controlled Fusion and Plasma Physics*, edited by C. Silva, C. Varandas, and D. Campbell (European Physical Society, Petit-Lancy, 2001), Vol. 25A, p. 613.
[32] K. G. McClements, Phys. Plasmas **12**, 072510 (2005).
[33] A. R. Polevoi, S. Yu. Medvedev, V. D. Pustovitov, V. S. Mukhovatov, M. Shimada, A. A. Ivanov, Yu. Yu. Poshekhonov, and M. S. Chu, *Proceedings of the 19th IAEA Fusion Energy Conference* (International Atomic Energy Agency, Vienna, 2003), CT/P-08.
[34] M. N. Rosenbluth and F. L. Hinton, Nucl. Fusion **36**, 55 (1996).
[35] H. R. Wilson, J.-W. Ahn, R. J. Akers, D. Applegate, R. A. Cairns, J. P. Christiansen, J. W. Connor, G. Counsell, A. Dnestrovskij, W. D. Dorland, M. J. Hole, N. Joiner, A. Kirk, P. J. Knight, C. N. Lashmore-Davies, K. G. McClements, D. E. McGregor, M. R. O'Brien, C. M. Roach, S. Tsaun, and G. M. Voss, Nucl. Fusion **44**, 917 (2004).
[36] J. D. Jackson, *Classical Electrodynamics* (Wiley, New York, 1975), p. 238.